

Comprehensive Summaries of Uppsala Dissertations
from the Faculty of Science and Technology 928



Mössbauer Spectroscopy of Meteoritic and Synthetic Fe-Ni Alloys

BY

YASSIR AHMED MOHAMED ABDU



ACTA UNIVERSITATIS UPSALIENSIS
UPPSALA 2004

Dissertation presented at Uppsala University to be publicly examined in Axel Hambergssalen, Geocentrum, Uppsala, Thursday, February 12, 2004 at 10:00 for the degree of Doctor of Philosophy. The examination will be conducted in English.

Abstract

Abdu, Y A. 2004. Mössbauer Spectroscopy of Meteoritic and Synthetic Fe-Ni Alloys. Acta Universitatis Upsaliensis. *Comprehensive Summaries of Uppsala Dissertations from the Faculty of Science and Technology* 928. 39 pp. Uppsala. ISBN 91-554-5854-8

This thesis reports on the results of investigating Fe-containing minerals in meteorites, with focus on Fe-Ni minerals and their magnetic properties, along with some synthetic Fe-Ni analogues. The New Halfa meteorite, which fell in Sudan 1994, has been studied using Mössbauer spectroscopy, X-ray diffraction, and electron microprobe analysis techniques, and classified as an ordinary L-type chondrite of petrologic type 4. Mössbauer spectra of taenite-enriched samples from the metal particles of the New Halfa (L4) and Al Kidirate (H6) meteorites identify the following γ (fcc) Fe-Ni phases: the ferromagnetic atomically ordered taenite (*tetrataenite*) with ~ 50 at % Ni, the ferromagnetic disordered taenite with ~ 50 at % Ni, the low-Ni (~ 25 at %) paramagnetic taenite (*antitaenite*). The presence of the superstructure of tetrataenite is confirmed by synchrotron X-ray diffraction.

Fe-rich γ (fcc) Fe-Ni alloys with compositions $\text{Fe}_{79}\text{Ni}_{21}$, $\text{Fe}_{76}\text{Ni}_{24}$, and $\text{Fe}_{73}\text{Ni}_{27}$, which serve as synthetic analogues of antitaenite, are prepared by mechanical alloying and subsequent annealing at 650 °C. The Mössbauer results indicate that these alloys are inhomogeneous and contain a high moment (HM) ferromagnetic Ni-rich phase (> 30 at % Ni) and a low moment (LM) paramagnetic Fe-rich phase, which orders antiferromagnetically at low temperature. The coexistence of these phases is attributed to phase segregation occurring on short range, probably nanometer scale, consistent with the Fe-Ni phase diagram below 400 °C where there is a miscibility gap associated with a spinodal decomposition in alloys with < 50 at % Ni.

The combined high field Mössbauer spectroscopy and SQUID magnetometry results on these alloys at room temperature indicate large induced local magnetic moments in the paramagnetic part of the sample, which increases with increasing the Ni content. The results, when compared with the high field Mössbauer results on antitaenite from the metal particle of Al Kidirate and New Halfa meteorites may be used to estimate the Ni content of antitaenite in meteorites.

High pressure ^{57}Fe Mössbauer spectroscopy measurements up to ~ 41 GPa have been carried out at room temperature using the diamond anvil cell (DAC) technique in order to investigate the magnetic properties of γ (fcc) $^{57}\text{Fe}_{53}\text{Ni}_{47}$ alloy. The results indicate a pressure induced Invar effect at ~ 7 GPa and a non-magnetic or paramagnetic state above 20 GPa, demonstrating the volume dependence of the magnetic moment of γ (fcc) Fe-Ni alloys.

Keywords: Meteorites, Tetrataenite, Antitaenite, Mössbauer spectroscopy, Mechanical alloying, Fe-Ni alloys, High pressure

Yassir Ahmed Mohamed Abdu, Department of Earth Sciences, Villav. 16, Uppsala University, SE-75236 Uppsala, Sweden

© Yassir Ahmed Mohamed Abdu 2004

ISSN 1104-232X

ISBN 91-554-5854-8

urn:nbn:se:uu:diva-3969 (<http://urn.kb.se/resolve?urn=urn:nbn:se:uu:diva-3969>)

To my parents

List of papers

This thesis consists of the present summary and the following papers:

- I Y. A. Abdu and T. Ericsson. Mössbauer spectroscopy, X-ray diffraction and electron microprobe analysis of the New Halfa meteorite, *Meteoritics and Planetary Science* 32 (1997) 373.
- II Y. A. Abdu, T. Ericsson, H. Annersten, N. A. Dubrovinskaia, L. S. Dubrovinsky and A. M. Gismelseed. Mössbauer studies on the metallic phases of Al Kidirate and New Halfa meteorites, *Hyperfine Interactions (C)* 5 (2002) 375.
- III Y. A. Abdu, T. Ericsson, and H. Annersten. Coexisting antiferromagnetism and ferromagnetism in mechanically alloyed Fe-rich Fe-Ni alloys: Implications regarding the Fe-Ni phase diagram below 400 °C, *Journal of Magnetism and Magnetic Materials* (In progress).
- IV Y. A. Abdu, H. Annersten, T. Ericsson, and P. Nordblad. Field induced local magnetic moments in γ (fcc) Fe-Ni anti-Invar alloys, *Journal of Magnetism and Magnetic Materials* (Submitted).
- V T. Ericsson, Y. A. Abdu, H. Annersten, and P. Nordblad. Non-magnetic stainless steels reinvestigated: A small effective field component in external magnetic fields, *Hyperfine Interactions C* (Submitted).
- VI Y. A. Abdu, H. Annersten, L. S. Dubrovinsky, and N. A. Dubrovinskaia. High pressure Mössbauer studies on fcc Fe₅₃Ni₄₇ alloy, *Hyperfine Interactions C* (Submitted).

Papers I and II are reprinted with kind permission of the publishers: The Meteoritical Society and Kluwer Academic Publishers.

Contents

1. Introduction.....	1
2. Mössbauer spectroscopy	3
2.1 Introduction	3
2.2 Hyperfine interactions	4
2.2.1. The isomer shift	4
2.2.2 Quadrupole splitting	5
2.2.3 Magnetic hyperfine splitting.....	5
2.3 Relative intensities of the Mössbauer lines	7
2.4 Other experimental techniques used with Mössbauer spectroscopy	8
2.4.1 X-ray diffraction (XRD).....	9
2.4.2 Superconducting quantum interference device (SQUID).....	9
3. Meteorites	10
3.1 Classification of meteorites	10
3.2 Fe-Ni alloys in ordinary chondrites.....	11
4. Mechanical alloying.....	17
4.1 Fe-Ni alloys produced by mechanical alloying.....	17
4.2 Antiferromagnetism of Fe-rich γ (fcc) Fe-Ni alloys.....	20
4.3 MA γ (fcc) Fe-rich Fe-Ni alloys in external magnetic fields	22
5. High-pressure Mössbauer spectroscopy	27
6. Concluding remarks.....	31
Summary in Swedish	33
Acknowledgements.....	36
References.....	38

1. Introduction

Iron (Fe) is probably the most abundant heavy element in the universe, where it scattered among the stars in our galaxy by supernova explosions. In the Earth's crust Fe ranks the fourth in abundance, after oxygen, silicon and aluminium. However, it is considered to be the major constituent of the core of the Earth and the other terrestrial planets. Meteorites, which were formed about 4.5 billion years ago and believed to come mostly from the asteroid belt between Mars and Jupiter, contain appreciable amounts of Fe occurring mainly as Fe(0) in metallic FeNi or as Fe(II) in the silicates and troilite (FeS). ^{57}Fe Mössbauer spectroscopy, due to its ability to give microscopic and differentiated information about the Fe atoms and their local environments, is one of the techniques that has been used successfully in studying Fe-containing minerals in meteorites. The study of meteorites in general can provide useful information concerning the formation and the early stages of our solar system.

The metal in meteorites is basically composed of two Fe-Ni minerals; *kamacite* with a body centered cubic (bcc) structure (the α -phase) and contains ~ 5 -7 at % Ni, and *taenite* having a face centered cubic (fcc) structure (the γ -phase) with ~ 25 -50 at % Ni. Taenite contains in its microstructure, which is formed below 400 °C during the extremely slow cooling of meteorites in their parent bodies, some extraordinary Fe-Ni phases that can not be produced in the laboratory by thermal treatment only. Mössbauer spectroscopy has played a major role in the study of Fe-Ni alloys from meteorites, e.g. the discovery of the atomically ordered $\text{Fe}_{0.5}\text{Ni}_{0.5}$ alloy, which was first observed in a taenite sample from the iron meteorite Cape York [1]. The new phase was later given the mineral name *tetrataenite* [2]. Danon *et al.* [3] were the first to identify tetrataenite in the metal particles of ordinary chondrites using Mössbauer spectroscopy.

Mössbauer spectroscopy of meteoritic taenite has also revealed the presence of another interesting fcc Fe-Ni phase with ~ 25 at % Ni referred to in the literature as the paramagnetic phase [1,4] or paramagnetic low-Ni taenite [5]. This phase, which is always observed in association with the ferromagnetic high-moment (HM) tetrataenite, has been reported by Rancourt and Scorzelli [6] to be a low-moment (LM) Fe-Ni phase. They also proposed the name *antitaenite* for this phase as a new meteoritic mineral

based on the antiferromagnetism of its synthetic analogues e.g. LM antiferromagnetic γ (fcc) Fe precipitates in Cu [6,7]. However, to our best knowledge, the antiferromagnetism of antitaenite has not yet been demonstrated experimentally.

Meteoritic Fe-Ni alloys have been used to determine experimentally the Fe-Ni phase diagram below 400 °C where atomic diffusion is very sluggish and there is a miscibility gap associated with a spinodal decomposition in alloys containing < 50 at % Ni [8]. The study of the microstructures in meteorites can also be used in tracing the cooling histories of meteorites in their parent bodies.

In this thesis we investigate the Fe-containing minerals in the ordinary chondrite, New Halfa, that fell in Sudan in the year 1994 (paper I). We developed a very simple method to extract the metal particles from ordinary chondrites and to obtain taenite-enriched samples in order to study tetrataenite and antitaenite. The method is applied to two chondrites, New Halfa and Al Kidirate (fell in Sudan in 1983) chondrites (paper II). We also produced by mechanical alloying some Fe-rich γ (fcc) Fe-Ni alloys (20 < at % Ni < 30), which serve as synthetic analogues of antitaenite. We investigate the magnetic properties of these synthetic alloys (papers III and IV) together with some LM γ (fcc) FeNiCr stainless steels (paper V), and the results are compared with that of meteoritic alloys. The main technique used in the above investigations is ^{57}Fe Mössbauer spectroscopy, in conjunction with other methods such as X-ray diffraction, electron microprobe analysis, and SQUID magnetometry. The study is of use for understanding phase transformations in the Fe-Ni system occurring at low temperature (below 400 °C), especially for fcc Fe-rich alloys. It is also related to the Invar and anti-Invar Fe-Ni alloys, which are of high technological importance. In this connection we also conducted high pressure Mössbauer experiments up to 41 GPa on HM ferromagnetic $\text{Fe}_{53}\text{Ni}_{47}$ alloy using Diamond Anvil Cell (DAC) technique (paper VI). The results show the ability of pressure in tuning the magnetic properties of materials, where on increasing pressure the $\text{Fe}_{53}\text{Ni}_{47}$ alloy becomes Invar and eventually a non-magnetic LM phase, showing a Mössbauer spectrum that resembles the spectra of antitaenite and mechanically alloyed Fe-rich alloys.

2. Mössbauer spectroscopy

2.1 Introduction

Mössbauer spectroscopy is a well-established technique that can provide valuable information in many areas of natural science. It is based on the Mössbauer effect, which is the recoilless resonant absorption of γ -rays by nuclei in a solid discovered by Rudolf Mössbauer in 1957. The recoilless resonant absorption of γ -rays, which was first observed by Rudolf Mössbauer in ^{191}Ir , has now been detected in tens of isotopes with ^{57}Fe being the most widely used. The probability of such a recoilless event known as the recoilless fraction or the f-factor depends on the γ -ray energy, temperature, and the vibrational properties of the solid in which the Mössbauer active nucleus is placed. In general, the recoilless emission and absorption is optimized for a low energy γ -ray with the nucleus tightly bound in a crystal lattice at low temperature.

The sharpness of the recoilless γ -ray energy is defined by the lifetime of the excited nuclear state through the Heisenberg uncertainty principle. Normally, the spread in energy, defined as the full width at half maximum intensity, is smaller in magnitude than the relatively weak interactions between the nucleus and the surrounding electrons (hyperfine interactions) [9]. This makes Mössbauer spectroscopy of primary importance as a mean of studying the hyperfine interactions using the nucleus as a probe.

In a conventional Mössbauer experiment a radioactive source containing the Mössbauer isotope in an excited state, e.g. radioactive ^{57}Co in Rh matrix for ^{57}Fe , is moving relative to an absorber consisting of the material to be investigated containing ^{57}Fe nuclei in the ground state. The emitted γ -ray energy, E_γ , (e.g. 14.4 keV for ^{57}Fe) then suffers a Doppler shift of $\Delta E = (v/c) E_\gamma$, where v is the source velocity and c is the velocity of light. For example, if $v = 1$ mm/s, ΔE is $\sim 10^{-8}$ eV, which is comparable to energy shifts and splittings of nuclear states caused by the hyperfine interactions ($\sim 10^{-7}$ eV). The Mössbauer spectrum thus obtained consists of a plot of the intensity of the γ -radiation transmitted through the absorber (or relative absorption) as a function of the source velocity. In ^{57}Fe Mössbauer spectroscopy a source

velocity in the interval ± 10 mm/s is enough to compensate for the shifts due to the hyperfine interactions.

2.2 Hyperfine interactions

The Mössbauer spectrum, which is described by the number, position, shape and relative intensity of the absorption lines, is governed by the nature of the different hyperfine interactions. These interactions perturb the nuclear energy levels and give rise to the hyperfine parameters: the isomer shift, the quadrupole splitting, and the magnetic hyperfine field.

2.2.1. The isomer shift

The isomer shift results from the electric monopole interaction between the nuclear charge distributed over a finite volume and the electronic charge density over that volume. It is caused by the difference in size of the nucleus in its ground and excited states. As a result of the monopole interaction the transition energy between the ground and excited states is modified (without splitting) relative to the isolated nucleus. The resulting Mössbauer spectrum consists of a single absorption line that is shifted from the position of zero velocity by the isomer shift. Being proportional to the electronic density at the nucleus, which depends on the electronic structure of the atom, the isomer shift can be used to determine the oxidation state of the Fe atom in a compound. However, what we really measure by Mössbauer spectroscopy is the centre shift (CS), which is the sum of the isomer shift (IS) and the second order Doppler shift (SOD), arising from the relativistic non-zero mean square velocity of the nuclei, i.e. $CS = IS + SOD$. Fig. 2.1 shows the effect of monopole interaction on the energy states and the corresponding Mössbauer spectrum. In ^{57}Fe Mössbauer spectroscopy the CS is usually measured relative to the CS of $\alpha\text{-Fe}$ at room temperature.

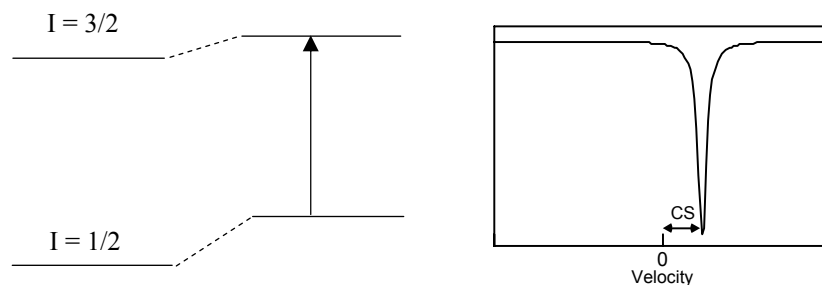


Fig. 2.1. The monopole interaction and the corresponding Mössbauer spectrum.

2.2.2 Quadrupole splitting

Any nucleus with a spin quantum number $I > 1/2$ has a non-spherical charge distribution characterized by a nuclear quadrupole moment. The electrostatic interaction between the nuclear quadrupole moment and the electric field at the nucleus created by the surrounding electric charges is called the electric quadrupole interaction. This interaction will give rise to a splitting of the nuclear energy state with $I > 1/2$ into substates without shifting the centre of gravity. For example, for ^{57}Fe the excited state ($I = 3/2$) will split into two substates characterized by $m_I = \pm 1/2$ and $\pm 3/2$ (m_I is the magnetic spin quantum number). The resulting Mössbauer spectrum is a two-line spectrum (doublet), with the positions of the two lines separated by the quadrupole splitting (QS), see Fig. 2.2. The quadrupole splitting can give valuable information regarding the symmetry of the bonding environment and the local structure around the Fe atom.

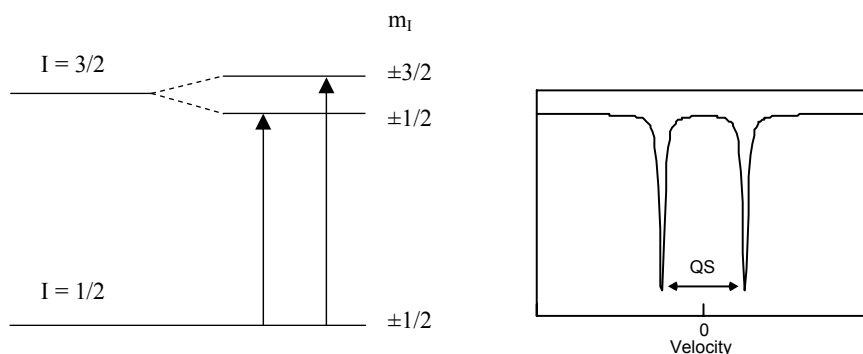


Fig. 2.2. The quadrupole interaction and the corresponding Mössbauer spectrum.

2.2.3 Magnetic hyperfine splitting

The magnetic hyperfine interaction is the interaction between the nuclear magnetic dipole moment and the magnetic field at the nucleus. This interaction fully raises the degeneracy of a nuclear state with $I > 0$ and splits it into $(2I + 1)$ substates. For ^{57}Fe , the ground state ($I = 1/2$) will split into two substates and the excited state ($I = 3/2$) into four substates. The allowed transitions between the substates of the ground and excited states lead to a Mössbauer spectrum with symmetric six lines (sextet), see Figs. 2.3 (a) and (b). The entire splitting of the absorption lines in the spectrum is proportional to the total magnetic field (B) at the nucleus.

The total magnetic field seen by the nucleus (the effective field) is the vector sum of the magnetic hyperfine field and the externally applied field. The main contribution to the magnetic hyperfine field comes from the Fermi contact interaction, which is a direct coupling between the nucleus and the unpaired s-electron density at the nucleus. The magnetic hyperfine fields are observed in the Mössbauer spectra of magnetically ordered materials or in paramagnets when the electronic spin relaxation time is longer than the Mössbauer time scale (~ 100 ns). For pure Fe, $B = 33.0$ T at room temperature, which corresponds to a total splitting of 10.62 mm/s. Analysis of magnetically split spectra can be used to investigate the magnetic ordering and magnetic structure of magnetically ordered materials.

There are cases where both the magnetic and quadrupole hyperfine interactions are present, resulting in very complex Mössbauer spectra. However when the quadrupole interaction is very small compared to the magnetic interaction, it can be treated as a small perturbation. The effect of such a small quadrupole perturbation in a magnetically split Mössbauer spectrum can readily be seen as an asymmetry in the sextet (see Fig. 2.3(b)). In this situation the quadrupole splitting (ΔQ) is defined by [10]:

$$\Delta Q = 1/2 [(V_6 - V_5) - (V_2 - V_1)]$$

where V_1, V_2, \dots, V_6 are the peak positions in the sextet.

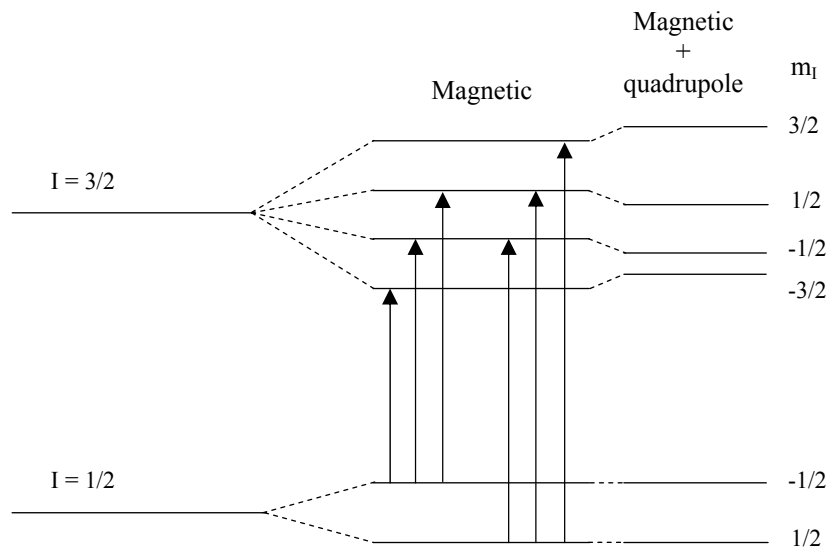


Fig. 2.3(a). The effect of magnetic interaction on the energy states of ^{57}Fe .

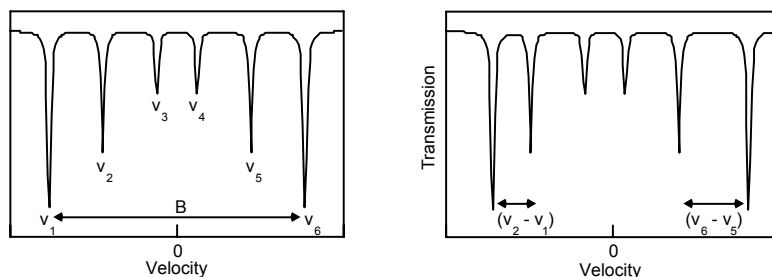


Fig. 2.3(b). The Mössbauer spectrum when the interaction is pure magnetic (left) and when there is a combined, magnetic + small quadrupole, interactions (right).

2.3 Relative intensities of the Mössbauer lines

As mentioned above, the magnitudes of the CS, QS, and B are determined from the position of the absorption lines only. The intensity of a particular hyperfine transition between, e.g. two nuclear substates I_1 and I_2 can be expressed as the product of two terms: (i) an angular dependent term which is averaged to unity in the case of a randomly oriented polycrystalline powder, where all orientations are equally probable. (ii) an angular independent term, where the intensity is proportional to the appropriate squared Clebsch-Gordan coefficients [9], i.e. Intensity $\propto \langle I_1 J - m_1 m \mid I_2 m_2 \rangle^2$, where m_1 and m_2 are the I_z values of the nuclear spins I_1 and I_2 , $J = I_1 + I_2$ and is called the multipolarity of the transition, and $m = m_1 - m_2$.

For $J = 1$ the transition is called a dipole, whereas for $J = 2$ it is a quadrupole transition. Most of the Mössbauer transitions are either magnetic dipole (M1) or electric quadrupole (E2). The selection rule for M1 is $m = 0, \pm 1$ and for E2 is $m = 0, \pm 1, \pm 2$. For example, although there are 8 transitions for the $1/2 \rightarrow 3/2$ M1, the $+3/2 \rightarrow -1/2$ and $-3/2 \rightarrow +1/2$ transitions are forbidden, and the remaining 6 transitions give an intensity ratio (for an ideal powder absorber) 3:2:1:1:2:3 for a magnetic hyperfine splitting (Fig. 2.3(b)). In the case of a quadrupole doublet the intensity ratio is 1:1.

Returning back to the angular dependent term let us consider the situation where the Mössbauer absorber of a magnetically ordered system is polarized by the application of an external magnetic field to give a specific direction of the internal field. The absorption intensities will then depend on the angle θ between the field direction and the direction of the γ -ray. For example if $\theta = 0^\circ$ the intensity ratio is 3:0:1:1:0:3 (see Fig. 2.4(a)) and if $\theta = 90^\circ$ it is 3:4:1:1:4:3 (see Fig. 2.4(b)).

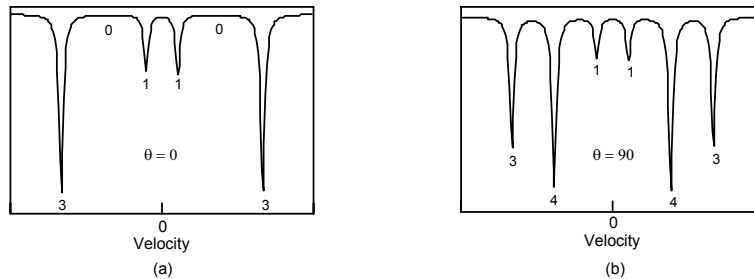


Fig. 2.4. Angular dependence of the relative intensities in the Mössbauer spectra when the angle (θ) between the applied magnetic field and the γ -ray direction is: (a) 0° and (b) 90° .

The total intensity of the absorption lines is the same, whether we have a singlet, doublet or a sextet spectrum, if the number of the Mössbauer atoms is the same [10]. This is because the total intensity depends on the f-factor, the number of Mössbauer atoms per cm^2 , and a nuclear factor. The intensity can then be used to estimate site occupancies for Fe-containing compounds.

Saturation of some absorption intensities may occur when using thick absorbers, which can also affect the relative line intensities. Even for thin powdered absorbers some materials show texture effects (preferred orientation) upon compression, resulting in relative intensities deviating from that of a random absorber. However, such textural effects can be avoided if we measure through the magic angle, 54.7° , being the angle between the normal to the absorber and the direction of the γ -ray [11]. Another effect that can also influence the relative absorption intensities is the Goldanskii-Karyagin effect arising from the anisotropy of the f-factor, however this effect is normally small.

2.4 Other experimental techniques used with Mössbauer spectroscopy

Mössbauer spectroscopy is a well-established method, however it is often necessary to combine it with other complementary techniques in order to obtain more reliable and complete information.

2.4.1 X-ray diffraction (XRD)

X-rays are diffracted when passed through a crystal, since their wavelengths are comparable to the separations of lattice planes ($\sim 1 \text{ \AA}$). The diffracted X-rays satisfy the Bragg law:

$$\lambda = 2 d \sin \theta$$

where λ is the wavelength of the X-ray photon, d is the lattice spacing, θ is the angle that the incident X-rays make with the lattice planes.

XRD is mainly used for structure and lattice constants determination, and hence for phase identification. However, other information such as electronic distribution around atoms, atomic ordering, lattice strain, etc can also be obtained.

2.4.2 Superconducting quantum interference device (SQUID)

The principle use of magnetometry is to measure the magnetization, whether it is intrinsic or induced by the field, of a material. One of the simple methods used for this purpose is the SQUID magnetometer. With magnetometry one can obtain results in a relatively short time on the total magnetic moment of the system and its variation with applied magnetic field and temperature. In contrast, Mössbauer spectroscopy can give an estimation of the local magnetic moment at the Fe nucleus.

In a SQUID magnetometry measurement, the sample is made to move in a constant magnetic field through superconducting pick-up coils connected to SQUID sensor. The change in the flux through the pick-up coils induces a current, which is converted into a detectable voltage that is proportional to the magnetic moment of the sample.

The SQUID magnetometer (Quantum Design MPMS) used in our studies is quite sensitive, thus only $\sim 50 \text{ mg}$ or less of the sample is needed for reliable results, and the instrument can be used from 4.2 K to 400 K in external fields up to 5.5 T.

3. Meteorites

Meteorites are particularly precious research materials because they represent samples (rocks and metal pieces) from inter-planetary space, which we have not yet been able to obtain through either manned or unmanned space missions. Thus, as a scientific resource, meteorites provide us with some of our first glimpses of the diverse array of planetary material scattered throughout the inner solar system. When meteorites enter the earth's atmosphere with a speed of 10 to 30 km/s the smallest of them are heated enough by friction to melt and glow, producing the spectacular streaks of light that we call shooting stars or meteors. The larger of these meteorites, which survive the flight and collide with Earth, undergo only surface melting forming what is called fusion crust that has a thickness of few millimeters [4]. However, the internal part of the meteorite is intact and quite often not harmed thermally.

3.1 Classification of meteorites

On the basis of their contents of metallic Fe-Ni and silicates, meteorites are classified into three major classes [12]:

- *Iron meteorites* (consist mainly of metal)
- *stony meteorites* (consist of silicates and minor metal)
- *stony-iron meteorites* (contain abundant metal and silicates)

Each of these three types of meteorites has extensive subdivisions, but we will be concerned mainly with the stony meteorites, which represent about 96 % of the observed falls. There are two types of stony meteorites: the *Chondrites*, undifferentiated meteorites, which contain mm-sized spheroidal objects called chondrules; and the *Achondrites*, differentiated meteorites that lack chondrules. The chondrites, which are the most common type of meteorites (~ 87 % of the falls), are further divided into three categories: *carbonaceous*, *enstatite*, and *ordinary* chondrites. The ordinary chondrites are classified into three chemical groups: H (high iron), L (low iron), and LL (low iron, low metal). Ordinary chondrites belonging to a specific chemical

group share common properties such as degree of iron oxidation, oxygen isotopic composition and major element chemistry, suggesting a single parent body for each group [13]. The three groups differ in their total iron contents ($H > L > LL$) and also in the ratio of oxidized to metallic iron ($LL > L > H$). The mineralogy of ordinary chondrites is dominated by the silicate minerals (olivine and orthopyroxene), subordinate Fe-Ni and troilite, and minor sodic plagioclase and diopside. Mössbauer spectroscopy is one of the techniques that has been used for investigating Fe-containing minerals in ordinary chondrites [14-16]. The absorption intensities of the different subspectra in a Mössbauer spectrum of a meteorite can be used to estimate the wt % of Fe-containing minerals present in the meteorite (**paper I**). Recently, Verma *et al.* [17] have found some systematics in the absorption areas of the Fe-containing minerals in ordinary chondrites that can be used in classifying these meteorites into the three groups H, L, and LL.

It is generally accepted that ordinary chondrites have experienced thermal metamorphism in their parent bodies (mostly asteroids) which is reflected in their textural and compositional variability. Within each chemical group there is a textural range from petrologic type 3 to type 7 indicating the degree of equilibration [12]. The H, L, and LL-group of ordinary chondrites with petrologic type 3 are called *unequilibrated* ordinary chondrites, where olivine and pyroxene show variable compositions, whereas ordinary chondrites with petrologic type 4 to type 7 are known as *equilibrated* ordinary chondrites. In equilibrated chondrites the compositions of olivine and pyroxene are relatively homogeneous and the degree of homogeneity increases with increasing petrologic number. The mole fractions of the iron end members of olivine (fayalite) and pyroxene (ferrosilite) are good criteria for the classification of equilibrated chondrites into the H, L, and LL groups [12]. (**paper I**)

3.2 Fe-Ni alloys in ordinary chondrites

The Fe-Ni metal in ordinary chondrites accounts for ~ 8-20 wt % of the bulk meteorite and occurs as grains varying in size from fine-grained to mm-sized spherical particles [18]. These grains are almost evenly distributed in a matrix, which is dominated by silicate minerals and troilite. There are two scenarios regarding the formation of metal grains in ordinary chondrites; that they are either remnants of a fractionated body, or they have formed *in situ* during thermal metamorphism that took place in the chondrites parent bodies [19].

The metal particles of some ordinary chondrites, iron and stony-iron meteorites contain in their microstructure special Fe-Ni phases, which are

formed below 400 °C as a result of the very slow cooling rate of these meteorites in their parent bodies. The estimated cooling rates for equilibrated ordinary meteorites lie in the range 0.1 to 100 °C/Ma [18]. Mössbauer spectroscopy has played a central role in the study of taenite in meteorites, where it gave the first conclusive evidence about the existence of tetrataenite with the $L1_0$ superstructure [1]. Tetrataenite is believed to be formed when meteorites cool very slowly below 320 °C, which is the order-disorder transition temperature [20]. It can occur as a single phase and it is considered as the only stable fcc Fe-Ni phase at low temperature [8]. Antitaenite, as evident from Mössbauer spectroscopy, has never been observed alone in meteorites. It always occurs in close microstructural association with tetrataenite as an epitaxial intergrowth, which was proposed by Rancourt and Scorzelli as a possible equilibrium state at ~ 20-40 at % Ni [6].

The study of these interesting phases in the metal particles of ordinary chondrites has been hampered by the presence of the silicates and troilite phases, which dominate the Mössbauer spectrum of the whole rock powdered samples (Fig. 3.1(a)). The method used in the literature to extract the metal particles from ordinary chondrites was normally utilizing conc. HF acid after subjecting the whole rock powdered sample to magnetic separation [3,5]. The use of HF acid at this stage is to dissolve the large amounts of silicates and troilite particles still attached to the metallic particles after the magnetic separation. Further treatment in HF will dissolve kamacite (the dominant phase) and leave the Ni-rich taenite minerals. However, dealing with conc. HF acid requires special precautions and sample handling. Also, conc. HF acid will attack the metal particles as well when it is used to separate them from the silicates and troilite, which makes the estimation of the wt. % of the metal particles in the meteorite difficult.

In **paper II** we have presented a very simple method for the extraction of the metal particles from the bulk sample in ordinary chondrites without using chemical treatment at this stage. The main idea lies on performing the magnetic separation in acetone. This is accomplished by first grinding the meteorite fragment into a powder using a mortar under acetone. The whole rock powdered sample is then subjected to magnetic separation (in acetone) using a hand magnet. The magnetic fraction is taken and submitted to further grinding and magnetic separation under acetone in order to purify the metal grains from silicates and troilite particles. This procedure of grinding and magnetic separation in acetone is repeated several times, depending on how the metal particles are cemented to the matrix, for further purification. In Fig. 3.1(b) we show the Mössbauer spectrum of the metal particles extracted from the Al Kidirate (H6) chondrite using this method. As seen from the figure, the spectrum contains only kamacite (the sextet), small amounts of

taenite (lie under the envelope of kamacite) and antitaenite (the singlet), and is free from the silicates and troilite phases.

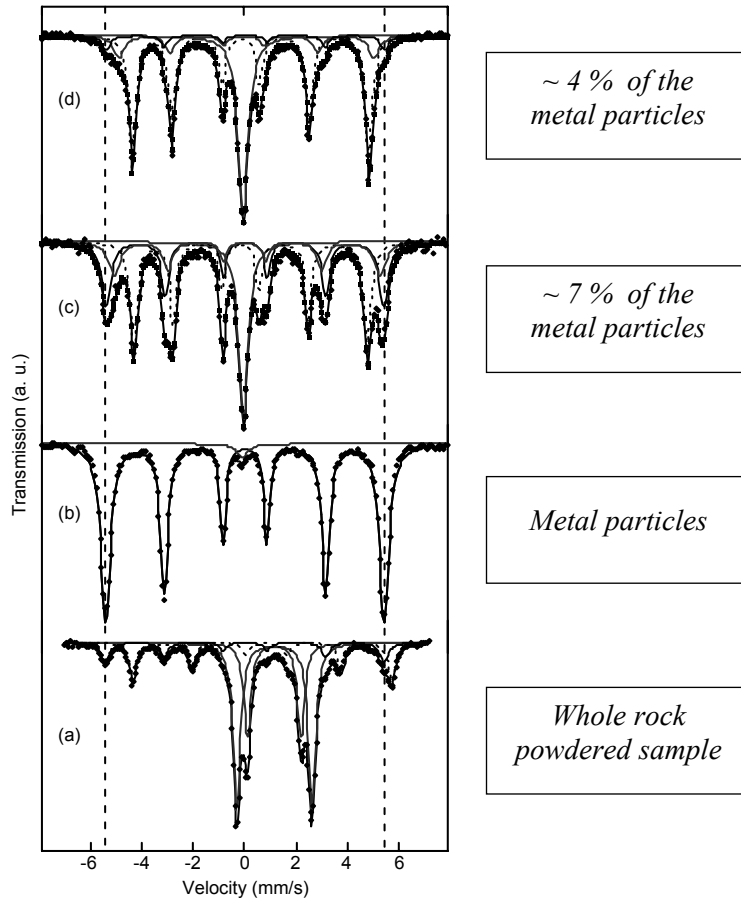


Fig. 3.1. Selected RT Mössbauer spectra from Al Kidirate meteorite. The vertical dashed lines mark the position of the outer peaks of kamacite. (a) inner doublet (pyroxene), outer doublet (olivine), sextet (troilite). In (b), (c), and (d): central singlet (antitaenite), dashed sextet (tetrataenite), solid sextet (disordered taenite).

In order to study taenite and to explore the presence of tetrataenite and antitaenite in the metal particles of ordinary chondrites, one has to get rid of kamacite, which usually dominates the Mössbauer spectra of the metal particles of ordinary chondrites (Fig. 3.1(b)). Kamacite can chemically be

dissolved using conc. HCl [21]. This is achieved by heating the purified metal particles in conc. HCl (e.g. 6M) at ~ 50 °C for a few hours. Figs. 3.1(c) and (d) show Mössbauer spectra of taenite-enriched samples representing ~ 7 % and 4 %, respectively, of the metal particles of Al Kidirate meteorite. The relative fraction of tetrataenite in sample (d) (~ 50 % in intensity) is surprisingly high, as the taenite content in this meteorite is too small not to be considered in fitting the Mössbauer spectrum of the whole rock powdered sample (Fig. 3.1(a)). Taenite is more abundant in the LL chondrites and decreases in abundance through the L to H chondrites where kamacite is most abundant [18].

In a taenite-enriched sample, tetrataenite can easily be identified by Mössbauer spectroscopy, where it exhibits an asymmetric six-line spectrum (see Fig. 3.1(d)). The asymmetry in the sextet is due to the quadrupole interaction arising from the non-cubic surroundings of the Fe atoms. The hyperfine magnetic field of tetrataenite was found to vary from meteorite to meteorite depending on the degree of order, e.g. for a well ordered tetrataenite $B \approx 28.5$ T and for a completely disordered $\text{Fe}_{0.5}\text{Ni}_{0.5}$ alloy $B \approx 31.1$ T [22]. The B values we have obtained for tetrataenite from Al Kidirate (H6) and New Halfa (L4) chondrites, 28.5 T and 28.6 T, respectively, indicate a high degree of order in tetrataenite in these meteorites (paper II). Antitaenite "Paramagnetic taenite", showing a single line Mössbauer spectrum, is also abundant in the taenite-enriched samples from these two meteorites (see Fig. 3.1(d) and paper II (Fig. 1)).

Tetrataenite and antitaenite have nearly identical lattice constants and thus they are not easily resolvable by X-ray diffraction (XRD) [4]. The superlattice reflections (extra reflections) of tetrataenite has been detected with XRD using Co K_{α} -radiation [1,23]. These reflections are very weak because Fe and Ni have almost similar scattering powers for X-rays. For example, although the taenite-enriched sample from Al Kidirate contains ~ 50 % of tetrataenite, we have not been able to detect the superlattice reflections of tetrataenite using Cu or Mo X-ray sources. However, using the high brilliance of synchrotron radiation, we were able to detect these extra reflections easily (Fig. 3.2). Fig. 3.3 shows the unit cell of the $L1_0$ superstructure of tetrataenite along with the lattice parameters (space group $P4/mmm$) of tetrataenite from Al Kidirate meteorite.

Beside tetrataenite and antitaenite, the Mössbauer spectra of taenite-enriched samples from Al Kidirate and New Halfa also show the presence of disordered taenite, fitted in paper II with two components; partially ordered taenite and completely disordered taenite. The occurrence of large amounts of disordered taenite together with tetrataenite has been interpreted as being due to shock or re-heating events [24].

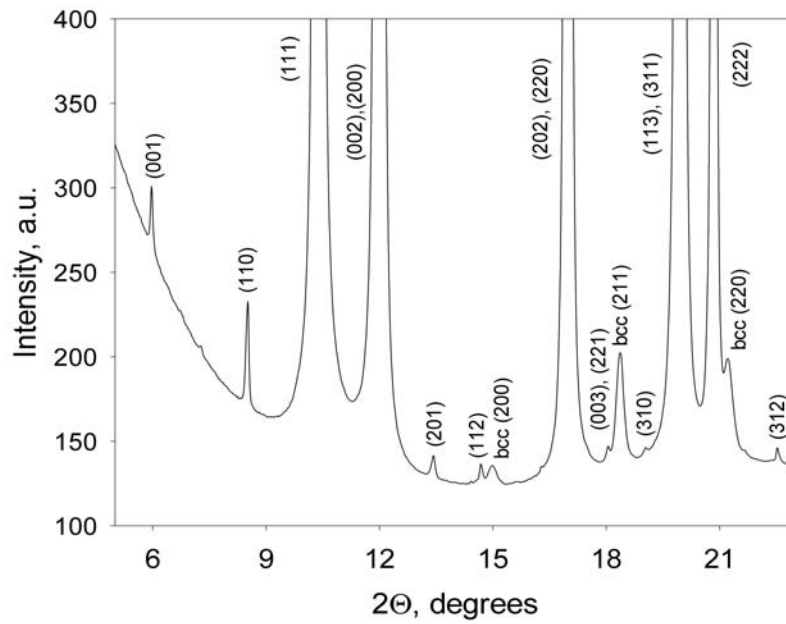


Fig. 3.2. Synchrotron powder X-ray diffraction pattern of taenite-enriched sample from Al Kadirate meteorite showing the superstructure lines (001), (110), (201), (112), (221), (003), (310), and (312) of tetrataenite, which also contributes to the strong fcc lines together with disordered taenite and antitaenite. The lines marked bcc represent the small amounts of kamacite in the sample.

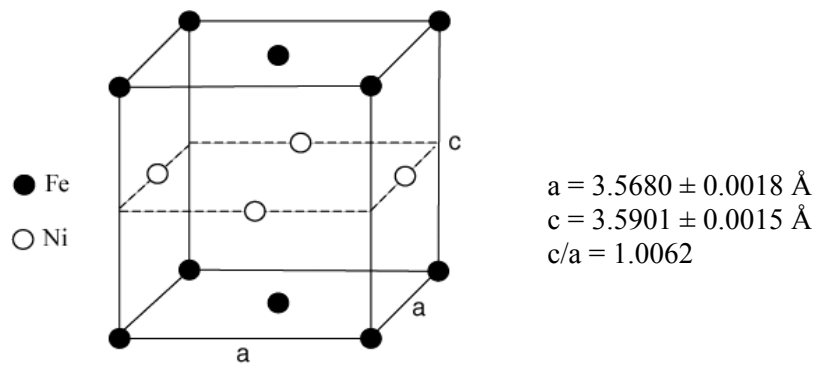


Fig. 3.3. The tetragonal unit cell of the L10 superstructure of tetrataenite [1]. Indicated are the lattice parameters of tetrataenite from Al Kadirate meteorite.

The fraction of disordered taenite in the taenite-enriched sample from New Halfa meteorite ($\sim 30\%$) can be correlated to a shock history, as we have estimated a shock of stage S3, 15-20 GPa [25], for this meteorite. This is in agreement with the Mössbauer study on a laboratory shocked meteoritic Fe-Ni alloy, where a shock of 20 GPa has increased the relative fraction of the disordered taenite from 12% to 42% on the expense of tetrataenite [26]. On the other hand, the taenite-enriched sample from Al Kidirate meteorite contains $\sim 15\%$ of disordered taenite, which may be due to kinetics. Furthermore, we attributed the small amounts of the α phase found in the taenite-enriched sample from New Halfa ($B = 33.9$ T, paper II) as being due to martensite. In this respect, it is worth to mention that the Fe-Ni alloy with $\sim 25\%$ Ni that we have observed in our microprobe analysis of the New Halfa meteorite (paper I), is in part due to martensite, especially for data points collected from single phase regions showing the above mentioned composition. Electron microprobe analysis, which has a resolution of $\sim 1\ \mu\text{m}$, can not resolve the nano-scale intergrowth of tetrataenite and antitaenite. However, it is possible to analyze these phases using analytical transmission electron microscopy (ATEM) [27].

4. Mechanical alloying

Mechanical alloying is a non-conventional method of material synthesis at low temperature, generally with non-equilibrium structures, by a dry and high-energy ball milling process, which involves transfer of material between the milled powders. The process starts with mixing the elemental powders in the appropriate proportion and loading the mixture into a steel vial together with some steel balls. The vial is then placed in a high-energy mill and vigorously agitated, producing collisions between balls or between vial and balls with impact speeds of the order of some m/s and shock frequencies of about some hundreds Hz [28]. In metallic systems, the particle size in alloys produced by mechanical alloying is generally in the micrometer scale. However, every particle contains a large number of nanograins, $\sim 10^6$ grains/ $(\mu\text{m})^3$, and thus can be regarded as a polycrystal with a high density of grain boundaries [28].

When a uniform material (e.g. pure metal or pre-alloyed sample) is subjected to ball milling, the process is called mechanical milling or mechanical grinding [29], which does not involve material transfer during milling. Mechanical milling is normally used to reduce the particle size of materials and to induce defects and phase transformations in solids.

Mössbauer spectroscopy has contributed significantly to the study of materials prepared by mechanical alloying [30]. It has been used in e.g. characterization of the milled products and nanostructured materials, study of phase transformations and order-disorder transformations that occur under milling, and understanding the mechanosynthesis of nanocrystalline materials.

4.1 Fe-Ni alloys produced by mechanical alloying

Since mechanical alloying produces large amounts of lattice defects in the material, which enhance atomic diffusion, it can be used to study phase transformations in the Fe-Ni system at low temperatures (below 400 °C) where atomic diffusion is practically zero. Xia *et al.* [31] studied the Ni-rich γ (fcc) Fe₆₀Ni₄₀ alloy prepared by mechanical alloying. The Mössbauer spectrum of the milled powder showed only a sextet with a distribution in

hyperfine fields characteristic of a disordered Fe-Ni alloy. When the milled powder was submitted to annealing at 350 °C for a long time, phase segregation into non-magnetic Fe-rich (< 30 at % Ni) phase (singlet subspectrum) and an atomically ordered $\text{Fe}_{0.5}\text{Ni}_{0.5}$ phase (with asymmetric sextet) has occurred.

Mechanical alloying has been used recently to suppress martensitic (fcc \rightarrow bcc) transformation in Fe-rich Fe-Ni alloys, resulting in γ (fcc) alloys after annealing of the milled powders in the stability region of the fcc phase and quenching them to room temperature [32,33]. However, to our knowledge, there is no systematic Mössbauer study on mechanically alloyed (MA) Fe-rich Fe-Ni alloys so far conducted.

In **paper III** we have prepared Fe-rich Fe-Ni alloys with compositions $\text{Fe}_{100-x}\text{Ni}_x$ ($x = 21, 24,$ and 27 at %) by mechanical alloying and studied their magnetic properties using variable temperature Mössbauer spectroscopy. The as-milled samples, characterized by X-ray diffraction and Mössbauer spectroscopy, contain a mixture of α (bcc) and γ (fcc) phases. However, annealing of the as-milled samples at 650 °C for 0.5 h and then quenching to RT resulted in a single γ (fcc) phase displaying a single line spectrum with similar hyperfine parameters to that of antitaenite (Fig. 4.1).

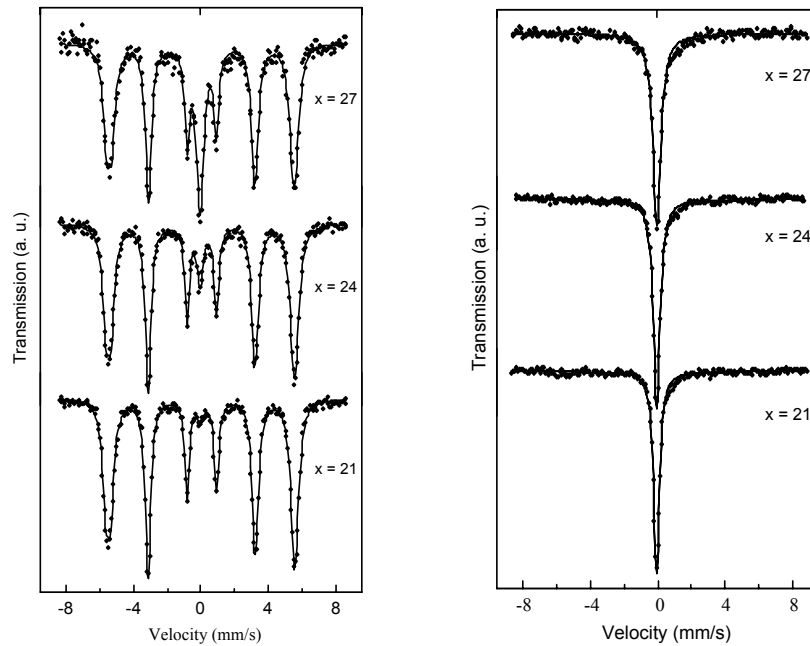


Fig. 4.1. RT Mössbauer spectra of MA $\text{Fe}_{100-x}\text{Ni}_x$ ($x = 21, 24,$ and 27 at %) alloys. Left: as-milled samples, sextet (bcc), singlet (fcc); right: after annealing at 650 °C.

To check the stability of these alloys against martensitic transformation, the samples were cooled in liquid nitrogen for a few minutes and then re-measured at room temperature by Mössbauer spectroscopy. As a result, the $x = 21$ sample was transformed partially to bcc martensite while the $x = 24$ and 27 samples remained in the γ (fcc) structure.

The low temperature Mössbauer spectra of annealed MA γ (fcc) $\text{Fe}_{73}\text{Ni}_{27}$ alloy show coexistence of a magnetically split pattern, with a hyperfine field of ~ 30 T, and a broad central singlet (Fig. 4.2). Besides, there is an intermediate field component ($B \sim 18$ T) introduced in the fitting to take care of the background bending. The magnetic sextet is assigned to a HM ferromagnetic Ni-rich phase with > 30 at % Ni and the singlet is attributed to a LM antiferromagnetic Fe-rich phase. The coexistence of these phases is interpreted as being caused by phase decomposition, probably in a nanometer scale, occurring as a result of the enhanced atomic diffusion in these mechanically alloyed samples.

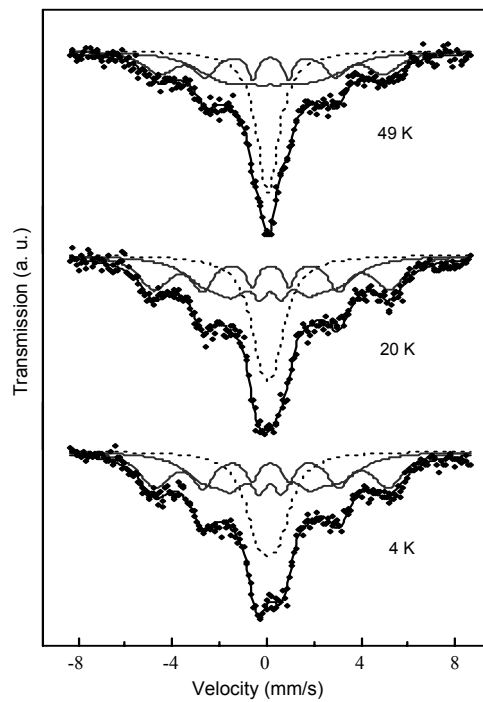


Fig. 4.2. Low temperature Mössbauer spectra of annealed MA $\text{Fe}_{73}\text{Ni}_{27}$ alloy.

Furthermore, upon warming up the sample to RT the magnetic sextet disappears, indicating that the small clusters of the Ni-rich phase behave in a way similar to the particle size effect in superparamagnetic materials. The amount of the ferromagnetic Ni-rich phase is found to increase with increasing nominal Ni concentration (relative intensity is $\sim 16\%$ and 35% for $x = 24$ and 27 , respectively). The phase segregation and the presence of the Ni-rich phase seem to play an important role in the stability of these alloys against martensitic transformation. The results and the arguments presented in paper III are in accord with the Fe-Ni phase diagram below $\sim 400\text{ }^\circ\text{C}$, where a miscibility gap associated with a spinodal decomposition occurs in γ (fcc) Fe-Ni alloys with < 50 at % Ni.

4.2 Antiferromagnetism of Fe-rich γ (fcc) Fe-Ni alloys

Kondorsky and Sedove [34], based on the measured temperature dependence of the magnetic susceptibility of γ (fcc) stainless steel ($\text{Fe}_{0.73}\text{Ni}_{0.09}\text{Cr}_{0.18}$), suggested that γ (fcc) Fe is antiferromagnetic. They also proposed that in ferromagnetic γ (fcc) Fe-Ni alloys there is a critical composition (~ 30 at % Ni) below which γ (fcc) Fe-Ni alloys are antiferromagnetic because of the negative exchange interaction between the neighbouring Fe atoms. In accordance with this Weiss [35], in his 2γ -state model, attributed the decrease in the Curie temperature with decreasing Ni content in the stability region of γ_2 (HM, ferromagnetic with ≥ 29 at % Ni) to the thermal excitation of γ_1 (LM, antiferromagnetic) which has a negative exchange interaction.

Using Mössbauer spectroscopy, the antiferromagnetic ordering in γ (fcc) Fe, stabilized as thin epitaxial films on a Cu substrate [36] or as small coherent precipitates in a Cu matrix [37] (both are paramagnetic at room temperature and show a single line Mössbauer spectrum) has been indicated by the drastic broadening of the Mössbauer linewidths at low temperatures. The hyperfine field ($\sim 2\text{-}3\text{ T}$) is not large enough to give a normal sextet in the Mössbauer spectrum. Determination of the Néel temperature (T_N) in these materials was achieved using either the "thermal scan" method [36,37], or by collecting Mössbauer spectra at different temperatures and then plotting the variation of linewidth with temperature [38, 39]. For example, using the thermal scan method, T_N for large γ (fcc) Fe precipitates in Cu was found to be 67 K [37].

In order to determine the ordering temperature in MA γ (fcc) $\text{Fe}_{76}\text{Ni}_{24}$ alloy, we have performed systematic variable temperature Mössbauer spectroscopy measurements on this alloy. The low temperature spectra display essentially the same features as that observed in annealed MA $\text{Fe}_{73}\text{Ni}_{27}$ alloy at low temperature, however the Ni-rich phase does not give a

clear magnetic sextet. The low temperature spectra of MA γ (fcc) $\text{Fe}_{76}\text{Ni}_{24}$ (below 78 K) are fitted with a singlet and two sextet components having a wide distribution of hyperfine fields. The value of B for the high field component is constrained to be equal to that of the alloy with $x = 27$ (i.e. 30 T), and we obtain a hyperfine field of ~ 10 T for the intermediate field component. By plotting the value of the linewidth of the singlet as a function of temperature, the paramagnetic to antiferromagnetic transition temperature was estimated to be ~ 40 K (Fig. 4.3).

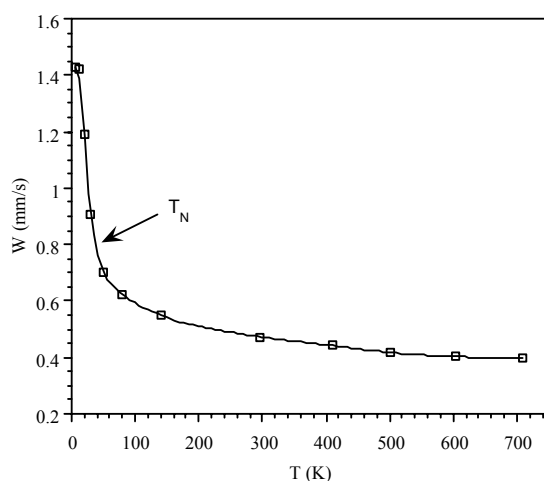


Fig. 4.3. Variation of the Mössbauer linewidth with temperature for the singlet subspectrum of annealed MA $\text{Fe}_{76}\text{Ni}_{24}$ alloy. The line through the data points is only a guide to the eye.

The results from paper III led us to conclude that meteoritic antitaenite is, at least in part, antiferromagnetic at low temperature. It also suggest that as a result of the extreme sluggishness of atomic diffusion in the Fe-Ni system below 400 °C, homogeneous fcc Fe-rich alloys have a tendency to transform to bcc martensite at low temperatures through a shear mechanism that requires no atomic diffusion. However, if the alloy is treated in a special way that can enhance atomic diffusion at low temperatures (< 400 °C), e.g. mechanical alloying, electron irradiation, then it can decompose into two fcc phases (Ni-rich and Fe-rich) as an alternative possibility towards thermodynamic equilibrium.

4.3 MA γ (fcc) Fe-rich Fe-Ni alloys in external magnetic fields

In **paper IV** we have studied MA γ (fcc) $\text{Fe}_{100-x}\text{Ni}_x$ ($x = 21, 24, \text{ and } 27$ at %) alloys using Mössbauer spectroscopy in external magnetic fields (up to 7 T) and SQUID magnetometry (up to 5 T) measurements at room temperature. The high field (3 - 7 T) Mössbauer spectra of the $x = 21$ and 24 alloys are fitted with two spectral components P_1 and P_2 with the relative intensity of lines 2 and 5 ($\Delta m = 0$ transitions) equal to zero (Fig. 4.4). The effective fields $B_{\text{eff}}(P_1)$ and $B_{\text{eff}}(P_2)$ for P_1 and P_2 , respectively, are found to depend almost linearly on the external field (B_{ext}), but with slopes that are smaller than unity, e.g. for the $x = 21$ alloy: $B_{\text{eff}}(P_1) \approx 0.92B_{\text{ext}}$ and $B_{\text{eff}}(P_2) \approx 0.61B_{\text{ext}}$. This indicates that the external magnetic field has induced a local magnetic moment, which gives rise to an induced hyperfine field ($B_{\text{ind}} = B_{\text{ext}} - B_{\text{eff}}$) that is opposite in direction to B_{ext} .

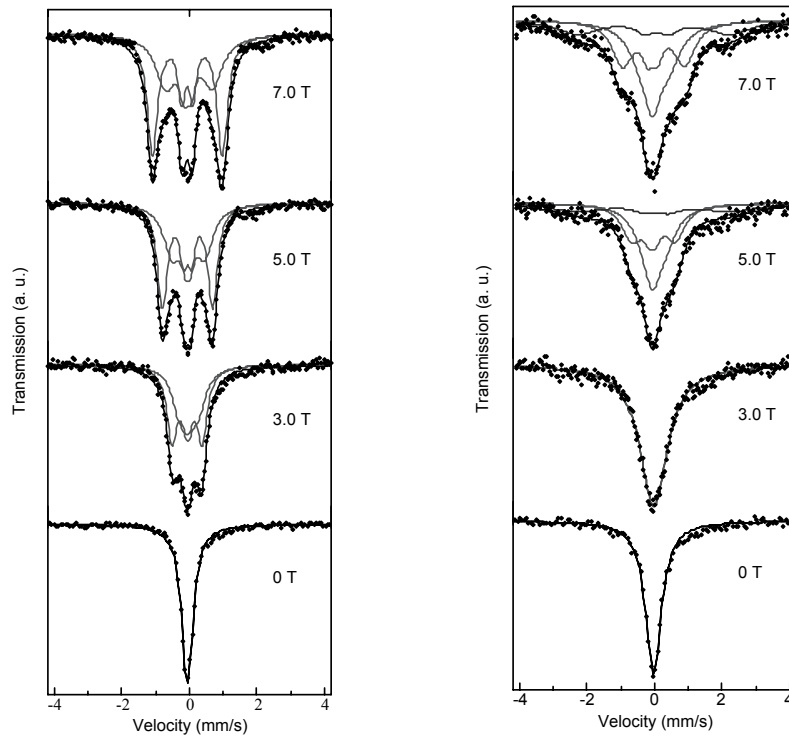


Fig. 4.4. RT Mössbauer spectra of the MA γ (fcc) $\text{Fe}_{79}\text{Ni}_{21}$ alloy (left) and $\text{Fe}_{73}\text{Ni}_{27}$ alloy (right) collected at different external fields applied parallel to the direction of the γ -ray.

The spectral component P_1 is assigned to the LM Fe-rich phase, which is paramagnetic at RT and orders antiferromagnetically at ~ 40 K. The component P_2 , which is also paramagnetic at RT, probably originates from Fe atoms in local environments with intermediate concentration of Ni.

The high field Mössbauer spectra of the $x = 27$ alloy show an additional component with an effective field that is larger than the applied field, e.g. at 7 T $B_{\text{eff}} \approx 14$ T which implies a hyperfine field of ≈ 21 T (Fig.4.4). We attributed this component to Ni-rich (> 30 at % Ni) clusters (domains) of a ferromagnetically ordered HM phase that behaves superparamagnetically at room temperature. This phase is also present in the $x = 21$ and 24 samples, but with decreasing amounts as concluded from our low temperature zero-field Mössbauer results (paper III). This is further supported by the RT magnetization (M-H) measurements, indicated by the non-linear character of the magnetization curves at low fields (Fig. 4.5).

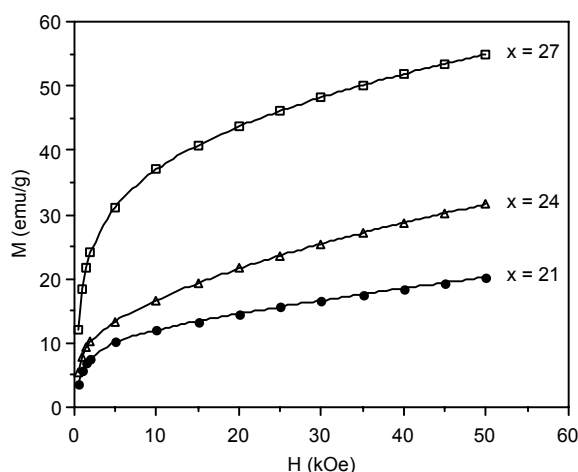


Fig. 4.5. Magnetization (M vs. H) plots of the MA γ (fcc) $Fe_{100-x}Ni_x$ ($x = 21, 24,$ and 27 at %) alloys at 295 K.

The magnetization curves also show a continuous linear increase of magnetization in the high-field region, which we have attributed as being due to the induced moments in the paramagnetic components P_1 and P_2 . There is a general agreement between the values of the induced moments, calculated from the weighted average induced hyperfine fields at 5 T and those estimated from the magnetization increment in the field range 2-5 T,

which supports the above argument. Therefore, the combined Mössbauer and magnetization results indicate induced hyperfine fields and hence induced moments in the paramagnetic components.

As natural analogues to our synthetic Fe-Ni alloys we have also studied antitaenite from the Al Kadirate and New Halfa meteorites using high field Mössbauer spectroscopy. The in-field Mössbauer spectra of antitaenite from these meteorites show essentially the same feature as that we observe in studied MA Fe-rich γ (fcc) Fe-Ni alloys, and are fitted also with two spectral components P_1 and P_2 (Fig. 4.6).

The induced hyperfine field and hence the induced moment in both P_1 and P_2 is found to increase with increasing the Ni content. This is evident from Fig. 4.7, where we plot the variation of the effective fields for P_1 with B_{ext} for MA Fe-rich γ (fcc) Fe-Ni alloys together with the data of antitaenite (at 6 T) from Al Kadirate and New Halfa meteorites. Note that $B_{\text{eff}} (P_1)$ is decreasing with increasing x , which implies that the induced hyperfine field and hence the induced magnetic moment is increasing with increasing the Ni content. Note also the large induced hyperfine field in antitaenite from New Halfa compared to that from Al Kadirate, which, when compared to the MA samples, might indicate a higher Ni content in the former. This may indicate different cooling histories for the two meteorites.

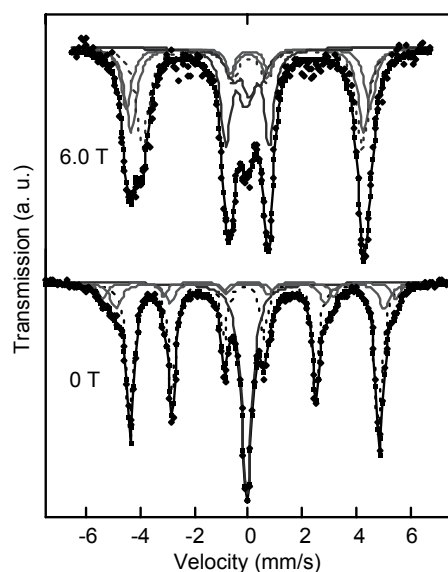


Fig. 4.6 RT Mössbauer spectra of taenite-enriched sample from Al Kadirate meteorite collected in zero-field (lower) and at 6.0 T (upper).

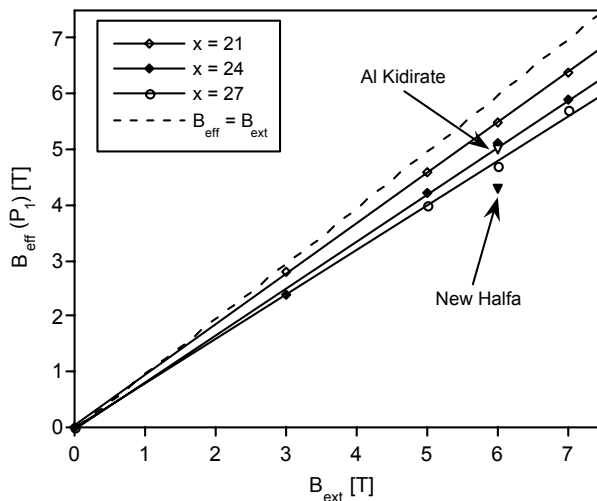


Fig. 4.7. $B_{eff}(P_\gamma)$ vs. B_{ext} for MA γ (fcc) $Fe_{100-x}Ni_x$ ($x = 21, 24,$ and 27 at %) alloys. The data points for antitaenite from Al Kidirate and New Halfa meteorites at 6.0 T are also shown.

In **Paper V** we have applied high field Mössbauer spectroscopy and SQUID magnetometry to three γ (fcc) Fe-Ni-Cr stainless steel samples; two powders with compositions (wt.%) $Fe_{70}Cr_{19}Ni_{11}$ and $Fe_{70}Cr_{17}Ni_{13}$, and a foil $Fe_{69}Cr_{18.5}Ni_{10.3}Mn_{1.8}$. The variable temperature Mössbauer spectra recorded in zero-field showed a singlet that is dramatically broadened below 50 K, indicating a paramagnetic to antiferromagnetic transition, also observed in our SQUID (M-T) curves, in agreement with the reported T_N values for antiferromagnetic stainless steels [34,37]. As for MA Fe-Ni samples, the in-field Mössbauer spectra of stainless steel are fitted with two quadruplet components, i.e. lines 2 and 5 missing in an ordinary sextet (Fig. 4.8). However, the high effective field component is nearly following the external field (i.e. $B_{eff} \approx B_{ext}$). On the other hand, the low field component gives an effective field of ~ 1 T that is almost independent of the external field. The results indicate that the samples can not be in a pure paramagnetic state at room temperature, and a possible interpretation could be a field-induced ferromagnetism.

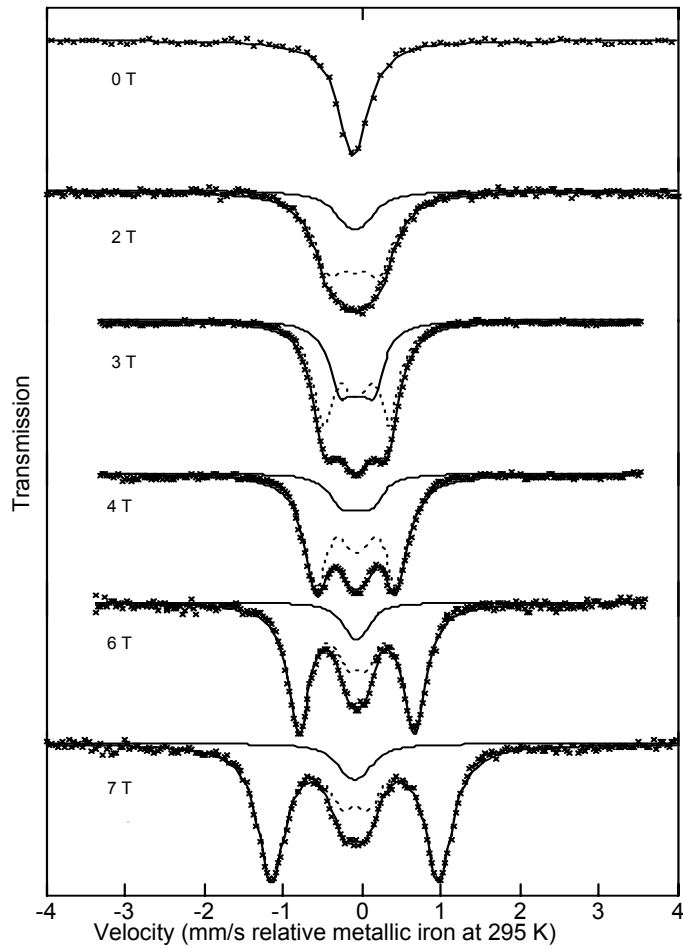


Fig. 4.8. Mössbauer spectra of the stainless steel $Fe_{69}Cr_{18.5}Ni_{10.3}Mn_{1.8}$ foil recorded at room temperature in longitudinal external fields. The spectra are fitted using two quadruplets (lines 2 and 5 missing in an ordinary sextet). The high field (dashed line) and low field (full line) components are also shown.

5. High-pressure Mössbauer spectroscopy

The primary effect of the application of pressure to a material is the reduction of the interatomic distances and hence the increase of atomic densities. This in turn will influence microscopic quantities such as the electronic density of states, bandwidths, and magnetic moments, and characteristic temperatures of a system, e.g. magnetic ordering temperature, superconducting transition, metal-insulator transition. Therefore, pressure allows the investigator to continuously tune the magnetic properties of materials.

Mössbauer spectroscopy is a valuable and powerful technique in studying pressure induced magnetic and structural phase transitions [40]. It has become particularly important with the innovation of the diamond anvil cell (DAC) and the ruby-fluorescence scale for pressure measurement, where pressures up to 100 GPa (~ 1 Mbar) can be achieved [41]. High pressure Mössbauer spectroscopy often gives unique information regarding magnetic properties at pressures above 10 GPa.

Ferromagnetic γ (fcc) Fe-Ni alloys with ~ 35 at % Ni show a near-zero thermal expansion coefficient in a wide temperature range (the Invar effect). The Invar effect and the associated anomalous physical properties have been a subject of intense theoretical and experimental research over a century, and many theoretical models have been proposed to explain its origin [35,42,43]. All these models predict a transition from a high moment or high-spin state at high volumes to a low moment or low-spin state at low volumes.

Abd-Elmeguid *et al.* [44] studied γ (fcc) $\text{Fe}_{68.5}\text{Ni}_{31.5}$ and $\text{Fe}_{65}\text{Ni}_{35}$ Invar alloys at variable temperatures down to 2 K and high pressures up to ~ 8 GPa by ^{57}Fe Mössbauer spectroscopy using B_4C anvils. Their results showed that above a critical pressure, e.g. ~ 5.8 GPa, the ferromagnetic state in $\text{Fe}_{68.5}\text{Ni}_{31.5}$ alloy is destroyed and the system displayed antiferromagnetic ordering at low temperatures. Dubrovinsky *et al.* [45] studied the pressure-volume relations in some fcc Fe-Ni alloys using high pressure XRD. They observed that Ni-rich alloys, which show positive thermal expansion at ambient pressure, become Invar systems around a certain pressure range, e.g. ~ 7 GPa for $\text{Fe}_{55}\text{Ni}_{45}$ alloy.

In **paper VI** we investigate the high pressure magnetic properties of the HM ferromagnetic γ (fcc) $^{57}\text{Fe}_{53}\text{Ni}_{47}$ alloy by ^{57}Fe Mössbauer spectroscopy

measurements up to ~ 41 GPa at room temperature using DAC. At ambient pressure, the Mössbauer spectrum of the alloy shows a six line magnetic pattern with an average hyperfine field of ~ 31 T with a distribution in hyperfine fields, characteristic of a HM ferromagnetic disordered alloy. As pressure increases (volume decreases) we observe Mössbauer spectra with an additional low hyperfine field component resembling spectra of γ (fcc) Fe-Ni Invar alloys (30-40 at % Ni), and eventually the hyperfine field breaks down at ~ 20 GPa and the alloy becomes non-magnetic showing only a single line Mössbauer spectrum (Fig. 5.1).

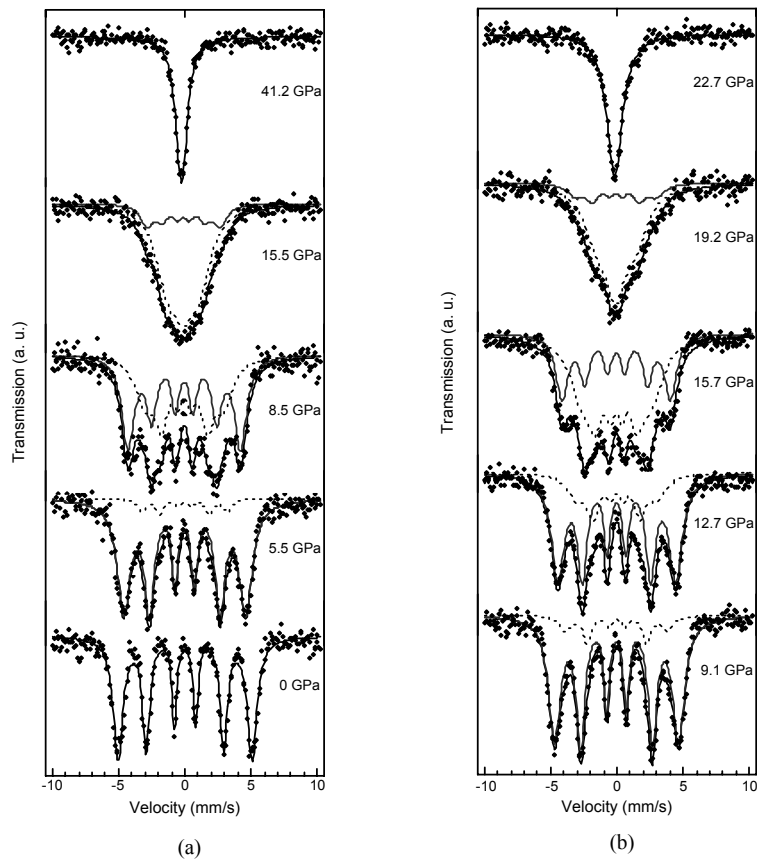


Fig. 5.1. High pressure Mössbauer spectra of $^{57}\text{Fe}_{53}\text{Ni}_{47}$ alloy collected at RT: (a) compression; (b) decompression.

The pressure dependence of the normalized weighted average hyperfine field, which is proportional to the average magnetic moment of Fe, indicates the instability of the magnetic moment of this alloy for pressures above ~ 2 GPa, showing a large negative pressure dependence as that observed in weak itinerant ferromagnetic Fe-Ni Invar alloys [44] (Fig. 5.2). The figure also shows pressure hysteresis in the pressure range $2 < \text{GPa} < 20$, where the average hyperfine field and hence the magnetic moment changes very fast. We observe a typical pressure induced Invar spectrum at ~ 7 GPa and ~ 12 GPa on compression and decompression, respectively. This is in agreement with high-pressure XRD studies on fcc Fe-Ni alloys, where a pressure induced Invar effect has been observed at 7.7 GPa around RT for $\text{Fe}_{55}\text{Ni}_{45}$ alloy on compression [45].

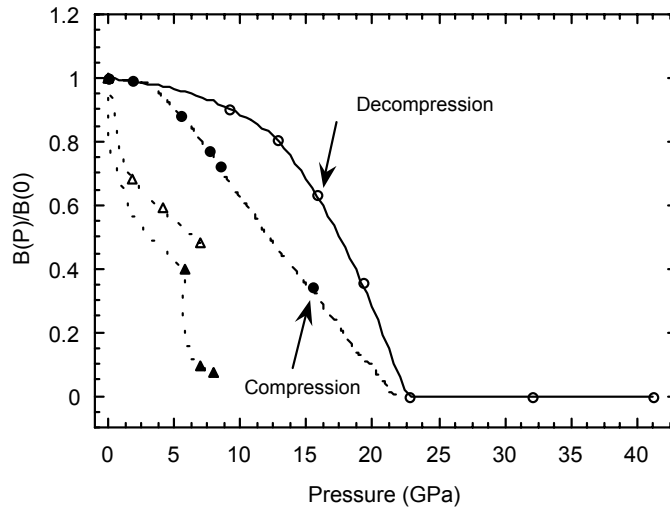


Fig. 5.2. Pressure dependence of the normalized weighted average hyperfine field for $^{57}\text{Fe}_{53}\text{Ni}_{47}$ alloy: filled circles (compression), open circles (decompression). Open and filled triangles represent data from ref. [44] (at 4.2 K) for Invar $\text{Fe}_{65}\text{Ni}_{35}$ and $\text{Fe}_{68.5}\text{Ni}_{31.5}$, respectively. The lines through the data points are only guides to the eye.

The centre shift (CS) decreases with increasing pressure as the volume decreases and hence the electron density at the Fe nucleus increases (Fig. 5.3). The sudden decrease in the CS at ~ 20 GPa may indicate a change in

the electronic configuration around Fe, e.g. a high-low spin state transition. Extrapolating the straight-line fit of the CS's above 20 GPa to 0 GPa gives a value of - 0.07 mm/s, which is very close to the CS's of MA γ (fcc) Fe-rich Fe-Ni alloys and antitaenite obtained at ambient conditions (**papers II and III**).

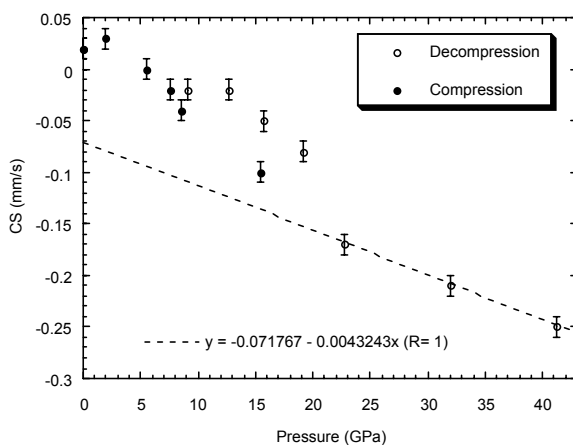


Fig. 5.3. Pressure dependence of the Mössbauer centre shift for $^{57}\text{Fe}_{53}\text{Ni}_{47}$ alloy. The dashed line is a linear fit to the CS's above 20 GPa.

The results obtained in **paper VI** agree quite well with theory and demonstrate the dependence of the magnetic moment on volume for γ (fcc) Fe-Ni alloys. It also shows the ability of pressure in tuning the magnetic properties of γ (fcc) Fe-Ni alloys, where by the application of pressure to a HM ferromagnetic alloy with 47 at % Ni we were able to observe Mössbauer spectra of Fe-Ni Invar alloys (30-40 at % Ni) and finally non-magnetic spectra of Fe-Ni anti-Invar alloys (< 30 at % Ni).

6. Concluding remarks

We have investigated the Fe-containing minerals in two stony meteorites that fell in Sudan, New Halfa (1994) and Al Kidirate (1983), and classified them as, respectively, L4 and H6 ordinary chondrites. A new simple method to extract the metal particles and to obtain taenite-enriched samples from ordinary chondrites is presented in this thesis. Taenite-enriched samples from Al Kidirate and New Halfa meteorites obtained by this method are found to contain tetrataenite and antitaenite with different proportions.

The application of Mössbauer spectroscopy to taenite-enriched samples of ordinary chondrites can give important clues regarding the thermal and mechanical histories of these meteorites. It will also shed light on the low temperature phase diagram in the Fe-Ni system on aspects such as kinetics of order-disorder, phase transformations at low temperature, which influence the magnetic properties of these technologically important alloys.

We have prepared and studied mechanically alloyed Fe-rich γ (fcc) $\text{Fe}_{100-x}\text{Ni}_x$ ($x = 21, 24, \text{ and } 27$ at %) alloys, which serve as synthetic analogues to meteoritic antitaenite. The RT Mössbauer spectra of these samples display only a singlet. From the low temperature Mössbauer results we found that these alloys are not homogeneous and contain a ferromagnetic HM Ni-rich phase (> 30 at % Ni) and a LM Fe-rich phase as a results of phase decomposition occurring on short range, probably nanometer scale. The LM phase, which is paramagnetic at room temperature, was found to order antiferromagnetically at ~ 40 K for MA γ (fcc) $\text{Fe}_{76}\text{Ni}_{24}$ alloy, suggesting that antitaenite is antiferromagnetic at low temperature. The small clusters (domains) of the HM Ni-rich phase behave superparamagnetically at room temperature, giving rise to a singlet. However, they display a non-linear behaviour in the magnetization curves at low fields, indicating that they are magnetically ordered at RT.

The high field Mössbauer results on MA γ (fcc) Fe-rich Fe-Ni alloys at RT indicate that large amounts of the sample is in the paramagnetic state, resulting in two spectral components with their effective fields almost linearly depend on the external field, but with slopes that are smaller than unity. This implies induced hyperfine fields and hence induced magnetic moments giving rise to a continuous increase of the magnetization in the high field region as seen by the SQUID magnetometer. The induced

hyperfine field and magnetic moment are found to increase with increasing the Ni content of the alloy. The in-field Mössbauer spectra of antitaenite from the New Halfa and Al Kidirate meteorites also show the same behaviour, which might be used to estimate the Ni-content in antitaenite.

The results of the high pressure Mössbauer study on fcc $\text{Fe}_{53}\text{Ni}_{47}$ alloy at RT, which indicate a pressure induced Invar effect at ~ 7 GPa and a non-magnetic or paramagnetic state at pressures above ~ 20 GPa, clearly demonstrate the volume dependence of the magnetic moment in fcc Fe-Ni alloys. This is in excellent agreement with theory. It would be of particular interest to further study the high pressure fcc phase obtained above 20 GPa in order to investigate its magnetic ground state and compare it with the high pressure phase of Fe (ϵ -Fe) which was found to have no local magnetic moments [46]. This can be achieved using variable temperature high-pressure Mössbauer spectroscopy in applied magnetic fields.

Summary in Swedish

Denna avhandling utgör studier av stenmeteoriter med speciell hänsyn till de metalliska mineralfaserna, huvudsakligen Fe-Ni-föreningar. Dessa har undersökts med Mössbauer spektroskopi, magnetometri, mikrosonanalys och röntgendiffraktion. Studierna har främst fokuserat på metallfasernas magnetiska egenskaper.

Meteoriter är objekt som kolliderat mot Jorden vilka oftast kan härledas från asteroidbältet mellan Mars och Jupiter. Dessa består av planetfragment och benämns efter deras olika mineralogisk sammansättning enligt följande:

- (i) stenmeteoriter (olivin, pyroxen, plagioklas, 8-20 vikts% metall)
- (ii) järnmeteoriter (huvudsakligen Fe-Ni-legeringar och troilit, FeS)

I avhandlingen har två stenmeteoriter (av typ ordinär kondrit), New Halfa och Al Kidirate, båda nedfallna i Sudan, undersökts. Resultaten visade att dessa innehöll (Fe, Mg)-olivin, (Fe, Mg)-pyroxen, plagioklas, troilit samt komplexa partier med olika sammansättningar av Fe-Ni-legeringar. Dessa utgör så kallade spinodala avblandningar, en kemisk segregering som är starkt beroende av den ytterst långsamma avkylningen som skedde efter planetkropparnas bildning. En metod för att anrika metallfasen ifrån silikatmineral har utvecklats för att med hjälp av Mössbauer spektroskopi närmare kunna karaktärisera de magnetiska egenskaperna hos de olika förekommande Fe-Ni-faserna. Följande faser har kunnat identifieras:

- (i) järnrik kamacit, < 10 at% Ni, bcc α -fas, ferromagnetisk (FM)
- (ii) taenit 25-50 at% Ni, fcc γ -fas, FM.

Taenit är ett mineral som visar sig ha komplex avblandningsstruktur, beroende på avkylningshastigheten. Tetrataenit, FM stökiometrisk ordnad FeNi med γ -fct struktur, har iakttagits i meteoriterna, tillsammans med oordnad taenit. En paramagnetisk (PM) γ -fcc Fe-Ni fas med ≈ 25 at% Ni - antitaenit - som alltid tycks uppträda tillsammans med tetrataenit har även kunnat identifieras med hjälp av Mössbauer spektroskopi.

Detaljerade studier av de magnetiska egenskaperna hos taenitfaserna har utförts på syntetiska analoga sammansättningar av $\text{Fe}_{100-x}\text{Ni}_x$, med $x = 21, 24$

och 27, med speciell fokus på PM fasen. För att stabilisera fcc-strukturen har metallblandningarna genomgått mekanisk malning med efterföljande upphettning i vakuum till 650 °C och därpå följande snabbkylning. Röntgendiffraktion visar att γ -fasen kan erhållas (meta)stabil under dessa syntesbetingelser. Mössbauer spektra uppvisar en singlett motsvarande den som observerats i antitaenite från meteoriterna.

För att bestämma den magnetiska ordningstemperaturen i aktuella FeNi-legeringar genomfördes systematiska Mössbauer mätningar vid låg temperatur. Under 78 K observeras i spektra från $\text{Fe}_{76}\text{Ni}_{24}$ två magnetiskt splittrade mönster med ett hyperfinfält på 30 respektive 10 T tillsammans med en allt bredare singlett. Vid ca 40 K inträder en dramatisk breddning av singletten. Detta indikerar en PM \rightarrow AFM (antiferromagnetisk) övergång. Förekomsten av de olika magnetiska ordningstemperaturerna tyder på en heterogen sammansättning och indikerar superparamagnetism hos avblandningar i nanostorlek med varierande Fe-Ni- förhållande.

Mössbauermätningar i yttre magnetfält (0 - 7 T) uppvisar en liknande uppdelning av singletten i två magnetiska signaler, P_1 och P_2 . Detta tolkas så att motsvarande järn atomer har av det yttre fältet inducerade magnetiska moment med motriktade hyperfinfält. Det magnetiska momentet ökar linjärt med Ni-halten och uppmättes för P_2 vid 5 T till 0.09, 0.15 och 0.18 μ_B/Fe . för $x = 21, 24$ och 27 respektive.

I frånvaro av yttre magnetfält tillskrivs P_1 järn med ett lågt magnetiskt moment i en Fe-rik omgivning, som ordnar sig AFM under 40 K. P_2 tillskrivs Fe med en intermediär Ni-omgivning som har ett hyperfinfält på ca 10 T vid låg temperatur. Ett magnetiskt mönster med ett hyperfinfält betydligt större än det yttre magnetfältet har observerats i $\text{Fe}_{73}\text{Ni}_{27}$. Det tillskrivs en Ni-rik fas (> 30 at-% Ni) med superparamagnetiska egenskaper vid rumstemperatur och ett hyperfinfält på ca 30 T vid låg temperatur.

Mätningar på prover från Al Kidirate och New Halfa i ett yttre magnetfält indikerar, i jämförelse med de syntetiska analogerna, en Ni-halt av cirka 25 respektive 30 at-% Ni i antitaenit.

Rostfritt FeCrNi-stål med sammansättningarna (i vikts%) $\text{Fe}_{70}\text{Cr}_{19}\text{Ni}_{11}$, $\text{Fe}_{70}\text{Cr}_{17}\text{Ni}_{13}$ och $\text{Fe}_{69,0}\text{Cr}_{18,5}\text{Ni}_{10,3}\text{Mn}_{1,8}$ har också studerats. Dessa vanliga kommersiella stålsorter har γ -fcc struktur på samma slag som ovanstående Fe-Ni legeringar. I likhet med antitaenit är dessa PM med en AFM övergång under 40 K. I yttre magnetfält vid rumstemperatur visar Mössbauerspektra två signaler, liknande P_1 och P_2 ovan. P_1 -signalen svarar mot ett ordinärt PM beteende medan P_2 -signalen indikerar ett av det yttre fältet inducerat, linjärt växande, magnetiskt moment.

Med hjälp av diamanttryckceller har en $\text{Fe}_{53}\text{Ni}_{47}$ legering (FM vid rumstemperatur och atmosfärstryck) undersökts in situ under höga tryck med hjälp av Mössbauer spektroskopi. Under tryck minskar hyperfinfältet och vid

20 GPa är legeringen omagnetisk. De observerade Mössbauer parametrarna indikerar att det paramagnetiska tillståndet inträffar samtidigt med en hög spin \rightarrow låg spin övergång i den undersökta legeringen. Detta kan förklaras med den stora volymismiskningen av kristallstrukturen som sker på grund av det höga trycket.

Acknowledgements

It has been a great pleasure to carry out my PhD studies at the Department of Earth Sciences, Uppsala University, and I am very grateful to everyone who has contributed one way or another to the accomplishment of this thesis. First, I would like to express my sincere gratitude to Prof. Hans Annersten, my supervisor, for giving me the opportunity to join his group and his continuous help and encouragement throughout these four years. I really appreciate your guidance and willingness to discuss at any time, as well as giving me the privilege to conduct my research in the direction I prefer.

I am very much grateful to Prof. Tore Ericsson, my co-supervisor, whom I know since 1995 when I first came to Uppsala to do part of my MSc program, where he supervised my work. Thanks a lot for your understanding, fruitful discussions and suggestions, and for your friendship and continuous support during my stay in Uppsala. I also thank his family, Astrid, Elin, and Karl-Einar for their hospitality and warm sympathy.

I would like to thank Docs. Örjan Amcoff, Per Nysten, Peter Lazor and Ala Aldahan for occasional consultation and useful discussions. My thanks are also extended to Profs. Sadoon Morad, Hemin Koyi, and Christopher Talbot, Docs. Genee Mulugeta and Håkan Sjöström. I would also like to thank Hans Harryson and Frank Westman for their skilled technical support.

My appreciation goes to Ms. Kersti Gløersen for her assistance with administrative matters. I appreciate your cheerful way of dealing with things and thanks for our French chats (*merci beaucoup!*).

My appreciation also goes to my colleagues-friends, Marcelo Ketzer, Abbas Bahroudi, Olga Shebanova, Alexey Shebanov, Tatyana Tentler, Johan Kjellman, Shawn Boye, Sara Sundberg, Sofia Carlsson, Khalid Al Ramadan, Mohamed Kalefa, Howri Mansurbeg, Erik Ogenhall, Faramarz Nilfouroushan, Osama Hlal, Abdulhadi Kulan, and Tomasz Sapota, for creating a nice atmosphere at work and for being sympathetic.

I would like to thank my office mate Dr. Ulf B. Andersson for creating a pleasant atmosphere, for discussions on different aspects of life and for teaching me how to skate (it was really a challenging experience!).

I also thank the staff of the Library of the Department of Earth Sciences, Uppsala University for being so co-operative in matters related to literature, and Taher Mazloomian at the *Geotryckeriet* for printing the thesis.

Special thanks go to Prof. Per Nordblad, Department of Engineering Sciences, Uppsala University, and Drs. Natalia Dubrovinskaia and Leonid Dubrovinsky, University of Bayreuth, Germany, for their collaboration and thoughtful discussions.

Prof. Lennart Häggström and Mr. Saeed Kamali from the Physics Department, Uppsala University, are thanked for their help in various ways and the nice company during Mössbauer conferences. I also thank Dr. Robert Delaplane and Ms. Jytte Eriksen, from the Studsvik Neutron Research Laboratory, for their help with mechanical alloying and for the good times we had during my visits to Studsvik.

My appreciation and thanks go to the Sudanese community and friends in Uppsala for sharing thoughts and for the glorious time we had together during our monthly gatherings, the list is so long but to name a few, Abdulbasit Alkundy, Abdelaziz Abdelkarim, Mohamed Kamal, Mohamed Eltahir, and Izzeldin Abugor. I acknowledge the executive committee of the Sudanese Society in Uppsala (SSU). I enjoyed playing football with our Sudanese team during summertime, and thanks to Babiker Elobeid (president of SSU) and Abdalla Elkhalfifa (team coach) for their efforts to maintain our football activity even in winter by playing indoors.

I would also like to thank my friends and former colleagues, Isam Salih & his family and Munir Abdalla & his family for their hospitality and concern during my stay in Sweden.

I acknowledge Mohamed Idris and Mohamed Abd Elbagi from the Geological Research Authority of the Sudan for kindly providing the sample of the New Halfa meteorite.

I would like to express my gratitude to my former supervisors Dr. Abbasher Gismelseed, my MSc supervisor, who first introduced me to the Mössbauer spectroscopy technique, for his valuable assistance and encouragement, Drs. Fathi El Khangi and Omer Ibrahim for their help and guidance during my employment at the Sudan Atomic Energy Commission (SAEC). I also extend my gratitude to all my former colleagues-friends at SAEC and Khartoum University.

I wish to thank Rifaat Kabbashi for his friendship, his noble hospitality during my visit to Nice, and for active contact in spite of the long distance.

Finally, my deepest and unlimited gratitude and respect go to my parents Ahmed and Alawia for their unconditional support and love, for their persistent encouragement throughout the different phases of my academic journey. My appreciation and admiration also go to my brothers Mohamed, Mutasim, Hadi, Salih, and my sister Awadia. Special thanks and regards to Shamael for her support, care, and inspiration during the final stages of writing the thesis.

References

1. J.F. Petersen, M. Aydin and J.M. Knudsen, *Phys. Lett.* 62A (1977) 192.
2. R.S. Clarke Jr. and E.R.D. Scott, *Am. mineral.* 65 (1980) 624.
3. J. Danon, R.B. Scorzelli, I. Souza Azevedo and M. Christophe-Michel-Lévy, *Nature* 281 (1979) 469.
4. J. M. Knudsen, *Hyp. Int.* 47 (1989) 3.
5. P. Kong, M. Ebihara, H. Nakahara, K. Endo, *Earth and Planet. Sci. Lett.* 136 (1995) 407.
6. D. G. Rancourt and R. B. Scorzelli, *J. Magn. Magn. Matter.* 150 (1995) 30.
7. D. G. Rancourt and R. B. Scorzelli, *American Mineralogist* 81 (1996) 766.
8. K.B. Reuter, D.B. Williams, and J.I. Goldstein, *Metall. Trans.* 20A (1989) 719.
9. T.C. Gibb: *Principles of Mössbauer spectroscopy*, Chapman and Hall, London 1976.
10. T. Ericsson: *Mössbauer in Uppsala*, Uppsala University, Department of Physics, 2000.
11. T. Ericsson and R. Wäppling, *J. de Physiq.* 37 (1976) C6-719.
12. R.T. Dodd: *Meteorites*, Cambridge University Press, 1981.
13. M. Trieloff, E.K. Jessberger, I. Herrwerth, J. Hopp, C. Fiéni, M. Ghélis, M. Bourot-Denise and P. Pellas, *Nature* 422 (2003) 502.
14. A. Bonazzi, I. Ortalli, G. Pedrazzi, K. Jiang and X. Zhang, *Hyp. Int.* 70 (1992) 953.
15. Y. Zang, J. G. Stevens, Y. Li and Z. Li, *Hyp. Int.* 91 (1994) 547.
16. A. M. Gismelseed, F. Khang, A. Ibrahim, A. A. Yousif, M. A. Worthing, A. Rais, M. E. Elzain, C. K. Brooks and H. H. Sutherland, *Hyp. Int.* 91 (1994) 551.
17. H.C. Verma, K. Jee, and R.P. Tripathi, *Meteoritics and Planetary Science* 38 (2003) 963.
18. Brearly and Jones in: *Reviews in Mineralogy*, V. 36, p. 3-251, *Planetary Materials*, ed. J.J. Papike, 1998.
19. P. Kong and M. Ebihara, *Geochim. Cosmochim. Acta* 60 (14) (1996) 2667.
20. J.F. Albersen, *phys. Script.* 23 (1981) 301.
21. A. Aldahan, personal communication.
22. J.M. Knudsen, PhD thesis, University of Copenhagen, 1984.
23. J. Danon, R.B. Scorzelli, I. Souza Azevedo and K. Imakuma, *Physica Scripta* 21 (1980) 223.
24. R.B. Scorzelli, I. Souza Azevedo, I. Ortalli, G. Pedrazzi and A. Bonazzi, *Hyp. Int.* 83 (1994) 479, and references there in.
25. D. Stöffler, K. Keil, and E.R.D. Scott, *Geochim. Cosmochim. Acta* 55 (1991) 3845.
26. R.B. Scorzelli, I.S. Azevedo, J. Danon and M.A. Meyers, *J. Phys. F: Met. Phys.* 17 (1987) 1993.

27. H. Leroux, Jean-Claude Doukhan and C. Perron, *Meteoritics and Planetary Science* 35 (2000) 569.
28. G. Le Caer, P. Delcroix, S. Bégin-Colin and T. Ziller, *Hyp. Int.* 141/142 (2002) 63.
29. C. Suryanarayana, *Prog. Mater. Sci.* 46 (2001) 1.
30. S.J. Campbell and W.A. Kaczmarek, In: *Mössbauer Spectroscopy Applied to Magnetism and Materials Science*, eds. G.I. Long and F. Grandjean, Vol. 2, Plenum Press, New York, 1996, p. 273, and references there in.
31. S. K. Xia, R. B. Scorzelli, I. Souza Azevedo, E. Baggio-Saitovich and A. Y. Takeuchi, *Mater. Sci. Forum* 225-227 (1996) 453.
32. Yu.V. Baldokhin, V.V. Tcherdyntsev, S.D. Kaloshkin, G.A. Kochetov, Yu.A. Pustov, *J. Magn. Magn. Mater.* 203 (1999) 313.
33. S. D. Kaloshkin, V. V. Tcherdyntsev, Yu. V. Baldokhin, I. A. Tomilin, E. V. Shelekhov, *J. Non-Crystalline Solids* 287 (2001) 329.
34. E. I. Kondorsky and V. L. Sedov, *J. Appl. Phys.* 31S (5) (1960) 331.
35. R.J. Weiss, *Proc. Phys. Soc.* 82 (1963) 281.
36. W. A. A. Macedo and W. Keune, *Phys. Rev. Lett.* 61 (4) (1988) 475.
37. U. Gonser, C.J. Meechan, A.H. Muir, and H. Wiedersich, *J. Appl. Phys.* 34 (8) (1963) 2373.
38. W. Keune, R. Halbauer, U. Gonser, J. Lauer and D. L. Williamson, *J. Magn. Magn. Mater.* 6 (1977) 192.
39. J. W. Freeland, I. L. Grigorov, and J. C. Walker, *Phys. Rev. B* 57 (1) (1998) 80.
40. M.P. Pasternak and R.D. Taylor, In: *Mössbauer Spectroscopy Applied to Magnetism and Materials Science*, eds. G.I. Long and F. Grandjean, Vol. 2, Plenum Press, New York, 1996, p. 273, and references there in.
41. R.D. Taylor and M.P. Pasternak, *Hyp. Int.* 53 (1990) 159.
42. V.L. Moruzzi, P.M. Marcus, K. Schwarz and P. Mohn, *Phys. Rev. B* 34 (1986) 1784.
43. M. van Schilfgaarde, I.A. Abrikosov, and B. Johansson, *Nature* 400 (1999) 46, and references there in.
44. M.M. Abd-Elmeguid, B. Schleede, and H. Micklitz, *J. Magn. Magn. Mater.* 72 (1988) 253.
45. L.S. Dubrovinsky, N.A. Dubrovinskaia, I.A. Abrikosov, M. Vennström, F. Westman, S. Carlson, M. van Schilfgaarde, and B. Johansson, *Phys. Rev. Lett.* 86 (21) (2001) 4851.
46. S. Nasu, T. Sasaki, T. Kawakami, T. Tsutsui and S. Endo, *J. Phys.: Condens. Matter* 14 (2002) 11167.

Acta Universitatis Upsaliensis

*Comprehensive Summaries of Uppsala Dissertations
from the Faculty of Science and Technology*

Editor: The Dean of the Faculty of Science and Technology

A doctoral dissertation from the Faculty of Science and Technology, Uppsala University, is usually a summary of a number of papers. A few copies of the complete dissertation are kept at major Swedish research libraries, while the summary alone is distributed internationally through the series *Comprehensive Summaries of Uppsala Dissertations from the Faculty of Science and Technology*. (Prior to October, 1993, the series was published under the title “Comprehensive Summaries of Uppsala Dissertations from the Faculty of Science”.)

Distribution:

Uppsala University Library
Box 510, SE-751 20 Uppsala, Sweden
www.uu.se, acta@ub.uu.se

ISSN 1104-232X
ISBN 91-554-5854-8